Sensors and Materials, Vol. 34, No. 9 (2022) 3533–3541
MYU Tokyo

S & M 3058

Compact Wideband Implanted Antenna for Medical Device Radiocommunications Service, Long Term Evolution, Global System for Mobile Communications, and Wireless Medical Telemetry Service Band Biosensing Applications

Pei-Jung Tseng,[1] Ching-Fang Tseng,[2*] Xiang-Yi Zeng,[2]
Cheng-Hsing Hsu,[3] and Ming-Hao Chou[2]

[1]Department of Pathology and Laboratory Medicine, Taichung Veterans General Hospital,
1650 Taiwan Boulevard Sect. 4, Taichung 40705, Taiwan
[2]Department of Electronic Engineering, National United University,
No. 2 Lien-Da, Nan-Shih Li, Miaoli 36063, Taiwan
[3]Department of Electrical Engineering, National United University,
No. 2 Lien-Da, Nan-Shih Li, Miaoli 36063, Taiwan

(Received February 5, 2022; accepted September 9, 2022)

Keywords: implantable antenna, biosensor, implanted biotelemetry, wireless telemetry

A compact-implantable-antenna-based biosensor is presented for the Medical Device Radiocommunications Service (MedRadio) (401–406, 413–419, 426–432, 438–444, and 451–457 MHz), long term evolution (LTE) 700 (698–787 MHz), global system for mobile communications (GSM) 850 (824–894 MHz), GSM900 (880–960 MHz), and Wireless Medical Telemetry Service (WMTS) (1395–1400 MHz) band applications. The proposed antenna has a wide operating bandwidth and small size owing to the effective use of meandering strips on the radiator and ground plane. An optimal antenna biosensor with compact dimensions of 15 × 15 × 2.25 mm^3 is fabricated and measured in a skin-mimicking gel. The measured 10 dB return loss bandwidth ranged from 376 to 1411 MHz, effectively covering the MedRadio, LTE700, GSM850, GSM900, and WMTS bands. Furthermore, the measured return loss exhibited stable characteristics with varying temperatures of the contact tissue, making it suitable for implanted biotelemetry and other wireless telemetry applications.

1. Introduction

With the expanding variety of diagnostic, therapeutic, and biological monitoring functions, wireless implantable devices are receiving considerable attention as a means of obtaining physiological data from patients to improve their quality of life.(1) Various frequency bands are allowed for medical implants. In 1999, the United States Federal Communications Commission (FCC) and the European Radio Communications Committee (ERC) allocated the 402–405 MHz band for the Medical Implant Communication Service (MICS), which was then the most commonly used band for medical implant communications. Ten years later, the FCC established

*Corresponding author: e-mail: cftseng@nuu.edu.tw
https://doi.org/10.18494/SAM4039

ISSN 0914-4935

the Medical Device Radiocommunications Service (MedRadio) with a range of 401–406 MHz, which combined the MICS band (402–405 MHz) with two extra spectra (401–402 and 405–406 MHz) to replace the previous MICS band.[2] FCC also allocated other spectra (413–419, 426–432, 438–444, and 451–457 MHz) together with the 401–406 MHz band for diagnosis and treatment applications involving implantable medical devices and wearable devices. The 433.1–434.8/868–868.6/902.8–928/2400–2480 MHz industrial, scientific, and medical (ISM) bands are additionally allocated for biotelemetry in some countries.[3] The 608–614/1395–1400/1427–1432 MHz bands are approved by FCC for the Wireless Medical Telemetry Service (WMTS).

An antenna is a very important part of an implantable system, as it communicates the collected biological information to hospitals or health data centers. Some challenging problems in implant antenna design must be considered by engineers, such as realizing a small size and wide bandwidth and avoiding signal attenuation through tissues. A stacked planar inverted-F antenna (PIFA) structure has often been used to reduce the antenna size.[4,5] In addition, a meandering strategy has also been used to reduce the size of implant antennas. Liu *et al.* proposed an implantable antenna operating at 372–468 MHz, that was based on a meandering line and six open slots in the ground.[6] Although the antennas were compact in Refs. 4–6, their bandwidths were too narrow to match the complicated and widely varying dielectric properties of tissues in the human body.

To create a wideband compact antenna for biomedical applications, the meandering structure is a strong candidate for use in implantable antenna design. In this paper, a compact wideband implanted antenna with an operating bandwidth from 376 to 1411 MHz is proposed. The compact size of the proposed antenna is realized by using meandering structures of the radiating element and the ground plane. Then wideband operation can be achieved by appropriately tuning some antenna parameters. We examined the geometric parameters of the proposed implantable antenna necessary to meet the requirements. We also investigated the performances of the proposed antenna inside different tissues of the human body and at different environmental temperatures. Finally, the proposed antenna was implanted in a skin-mimicking gel to confirm its simulated and measured performances.

2. Antenna Design and Experimental Results

Figure 1 presents the geometry of the proposed wideband implantable antenna, which has dimensions of 15 × 15 × 2.25 mm^3. The antenna is printed on an FR4 substrate with a dielectric constant of 4.4, a loss tangent tanδ of 0.02, and a thickness of 1.6 mm and is fed by a microstrip line of width 3 mm. Two meandering strips, used as the radiating element [Fig. 1(a)] and ground plane [Fig. 1(b)], are placed on the top and bottom of the FR4 substrate, respectively. The meandering structure forces the current to flow near the two parallel meandering strip lines, increasing the current flow path, which decreases the resonant frequency and reduces the antenna's size. A broad impedance bandwidth can be obtained through suitable adjustment of the lengths of the meandering lines of the antenna element and ground plane. The similar current lengths of the radiating element and ground plane can generate two close resonant frequencies.[7,8] Single-layer homogeneous skin tissue with dimensions of 100 × 100 × 24 mm^3 is used for

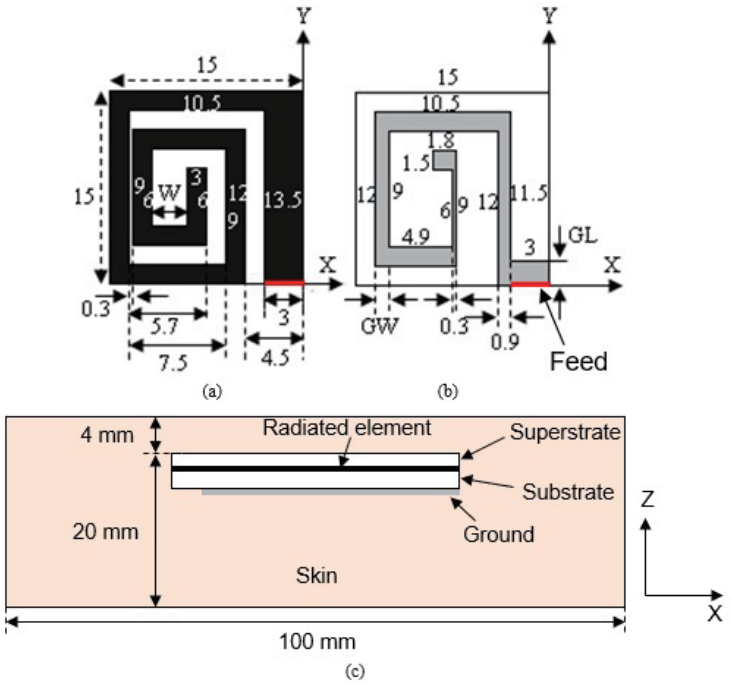

Fig. 1. (Color online) Geometry of the proposed antenna: (a) radiating element, (b) ground plane, and (c) side view of the implanted antenna inside a single-layer skin tissue model.

simulation. The proposed antenna is embedded at a depth of 4 mm from the skin surface. The skin tissue model is placed in the center of a radiation boundary box having dimensions of 300 × 300 × 300 mm^3. The physical simulation model of the proposed implantable antenna is illustrated in Fig. 1(c). During the simulation process, the dielectric constant (ε_r) and conductivity (σ) of the skin tissue model are respectively set at 46.7 and 0.689 S/m and at 41.4 and 0.867 S/m for frequencies of 402 and 902 MHz, respectively.[9] The proposed antenna has a similarly good performance when embedded in a single-layer skin tissue model for both frequencies. Therefore, the subsequent simulation results are only given for a frequency of 402 MHz. Al_2O_3 with a permittivity of 9.8 and a height of 0.65 mm is used for the superstrate, and its dimensions are shown in Fig. 1.

To clarify the effect of the two meandering strips, we simulate the proposed antenna with different values of parameters *W*, *GL*, and *GW* (see Fig. 1), the simulated S_{11} results of which are shown in Figs. 2–4, respectively. Figure 2 shows the simulated return loss curves as a function of width *W*. *W* affects the coupling capacitance between the upper radiator element and the ground plane. Accordingly, impedance matching can be realized. The optimal impedance bandwidth below −10 dB is in the frequency range of 359–1953 MHz when *W* = 2.7 mm.

The effect of the parameter *GL* on the return loss performance of the proposed antenna is simulated, as illustrated in Fig. 3. It can be observed that the lower resonances do not change significantly with increasing *GL*, while the upper resonances become weak. However, the resonant frequencies do not significantly shift. Therefore, we use the minimum value of *GL* to obtain the desired impedance-matching performance. Figures 2 and 3 show that impedance matching is easily realized by controlling *W* and *GL*.

Figure 4 shows the simulated S_{11} as a function of *GW*. With increasing *GW*, resonant frequencies f_2 and f_4 clearly shift to higher frequencies, while f_3 shifts to a lower frequency. By adjusting *GW*, the frequency shift can be compensated to fit the variations of lossy tissue environments for real implantable applications.

Figure 5 shows simulated and measured S_{11} for the antenna embedded in a human-skin-mimicking gel for the MedRadio 402 band. The composition of the gel for the MedRadio 402 band is taken from Ref. 10. The concentrations of the ingredients in our skin-mimicking gel prepared for the MedRadio 402 band are 55.92% sugar, 2.53% NaCl salt, and 41.55% deionized water to form a 100 ml solution. Then, 1 g agarose is added to the solution. The skin-mimicking gel is housed in a plastic container with dimensions of 100 × 100 × 24 mm^3. The proposed antenna is implanted at a depth of 4 mm inside the skin-mimicking gel. We obtained ε_r of 46.37 and σ of 1.22 S/m for the skin-mimicking gel. From Fig. 5, it can be seen that the measured curve agrees well with the simulated one in the MedRadio 402 band (f_1). As expected, the measured resonant frequencies f_2, f_3, and f_4 shift to lower values owing to the higher ε_r of the skin-mimicking gel prepared for the MedRadio 402 band. In addition, there is some disagreement

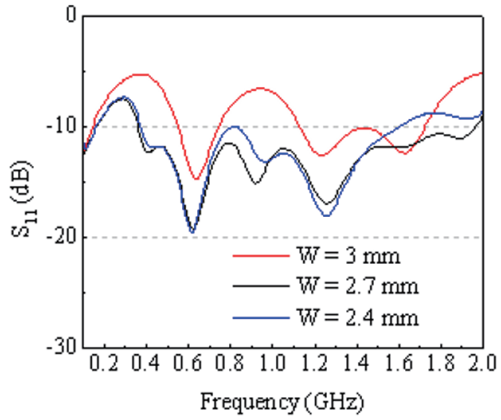

Fig. 2. (Color online) Simulated S_{11} as a function of parameter *W*.

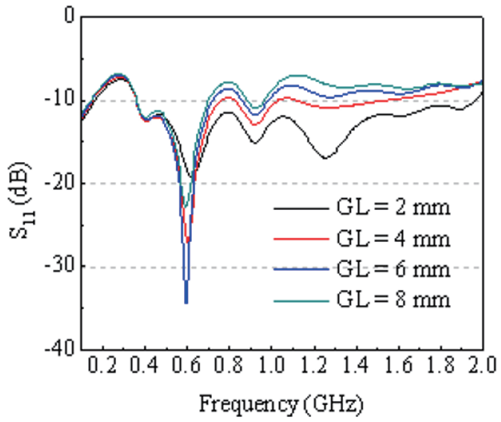

Fig. 3. (Color online) Simulated S_{11} as a function of parameter *GL*.

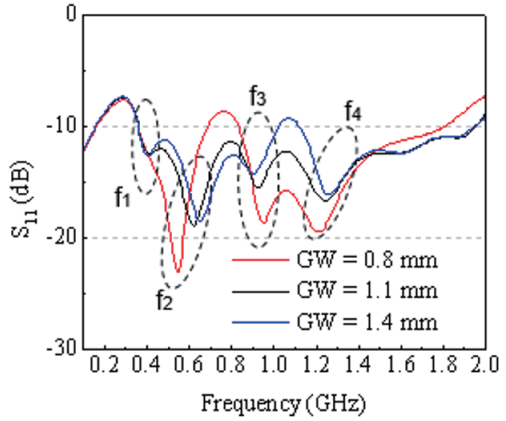

Fig. 4. (Color online) Simulated S_{11} as a function of parameter *GW*.

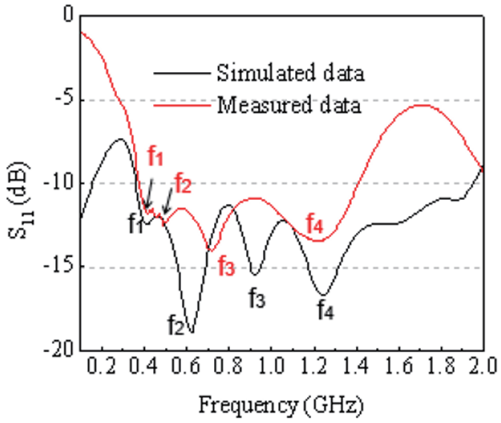

Fig. 5. (Color online) Simulated and measured S_{11} for the proposed antenna.

between the measured data and simulated results, especially in the higher frequency band. This discrepancy is due to the conductivity (σ = 1.22 S/m) of the prepared skin-mimicking gel being higher than that of real skin. The phenomenon is similar to that in Ref. 10. As seen from the graph, the measured bandwidth in the skin-mimicking gel is 1035 MHz (from 376 to 1411 MHz) for S_{11} less than −10 dB.

Figure 6 shows the simulated return losses of the proposed antenna immersed in skin, eye tissue, muscle, and heart. Regardless of the biological tissue in which the proposed antenna is implanted, the MedRadio, long term evolution (LTE) 700, global system for mobile communications (GSM) 850, GSM900, and WMTS bands are still covered and a wide bandwidth from 377 to 1680 MHz is obtained.

With an increase in temperature from 36 to 40 ℃ at 400 MHz, the dielectric constant and conductivity of the human body tissue slightly decrease and increase, respectively.[11] To understand the influence of the temperature change of the skin tissue on the proposed implanted antenna, we used a heating plate to control the temperature of the skin tissue model. Figure 7 presents the measured return losses of the proposed antenna in the skin-mimicking gel at different temperatures. From the results, one can observe that the temperature effect on the proposed antenna implanted in the skin-mimicking gel is minimal because of minimal changes in permittivity and conductivity upon varying the temperature from 36 to 40 ℃.

Figure 8 shows the radiation gain patterns of the proposed antenna implanted in the skin-mimicking gel. The amount of radiation reaching the human body is less than 10 dBi, meaning that the power is delivered outward from the body. The measured peak gains are −20.9, −14.6, −13.2, −12.9, and −11.8 dBi for operation at 403, 700, 850, 900, and 1400 MHz, respectively. Owing to the gain of the implanted antenna being greater than −35 dBi, the proposed antenna has a beneficial design for wireless biological data telemetry applications.

Table 1 gives the performances of skin-implantable antennas operating with the MedRadio system.[12–16] In our work, the proposed antenna has a slightly larger volume because of the low

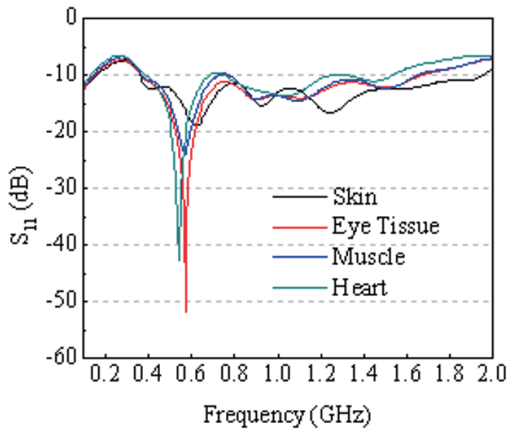

Fig. 6. (Color online) Simulated S_{11} for the proposed antenna implanted in different biological tissues.

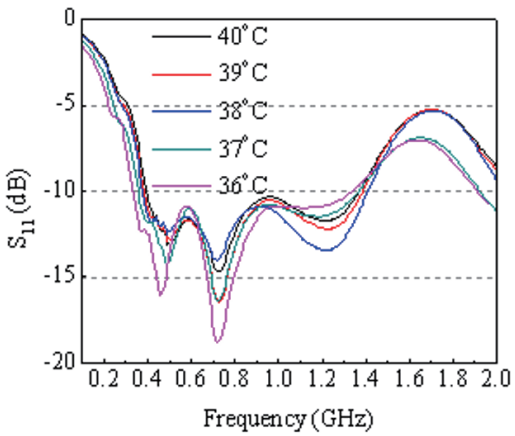

Fig. 7. (Color online) Measured S_{11} of proposed antenna implanted in skin-mimicking gel at different temperatures.

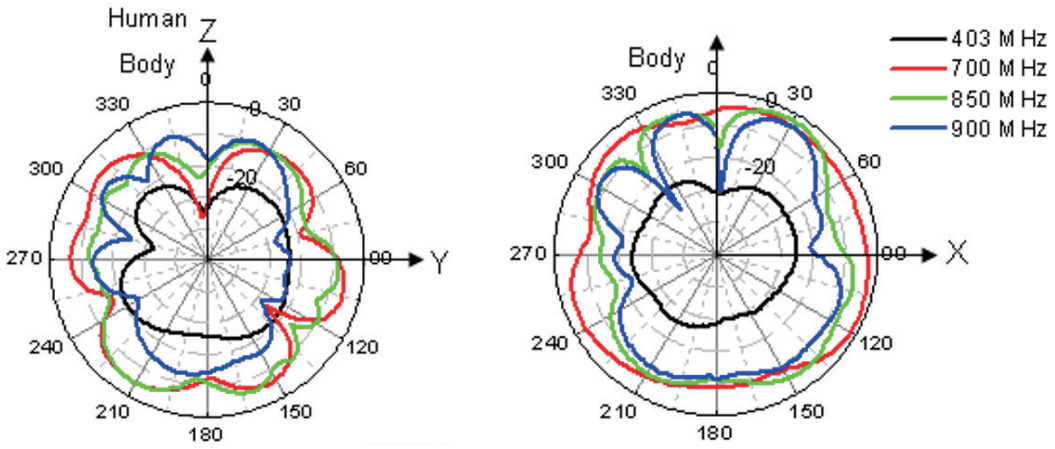

Fig. 8. (Color online) Measured radiation gain patterns of the proposed antenna implanted in the skin-mimicking gel. (a) *Y*–*Z* plane; (b) *X*–*Z* plane.

Table 1
Performances of the proposed implantable antenna and these in previous studies (thickness unit: mm).

Ref.	12	13	14	15	16	This work
Bandwidth (MHz)	360–620 2320–2540	356–504 2316–2529	280–480 2400–2480	375–475 2200–2500	373–525 2430–2600	376–1411
Volume (mm^3)	153.35	17.15	447.04	248.92	49.5	506.25
Implantation depth	Skin/3 mm	Skin/3 mm	Skin/3 mm	Skin/3 mm	Skin/3 mm	Skin/4 mm
Peak gain (dBi)	M: −38.08 I: −22.03	M: −30.5 I: −18.2	M: −18.5 I: −19.5	M: −46 I: −19	M: −38.8 I: −18.6	M: −20.9 L: −14.6 G8: −13.2 G9: −12.9 W: −11.8
Shorting pin used	Yes	No	No	Yes	Yes	No
Substrate	Rogers 3010	Rogers 6010	Rogers 3210	Rogers 3010	Rogers 3010	FR4
ε_r	10.2	10.2	10.2	10.2	10.2	4.4
thickness	0.635	0.25	1.27	0.635	0.25	1.6
Superstrate	Rogers 3010	Rogers 6010		Rogers 3010	Rogers 3010	Al_2O_3
ε_r	10.2	10.2	None	10.2	10.2	9.8
thickness	0.635	0.127		0.635	0.25	0.65

M: MedRadio, I: ISM, L: LTE700, G8: GSM850, G9: GSM900, W: WMTS

permittivity of the substrate and superstrate. However, compared with the antenna in Ref. 14, the proposed antenna has a compact volume when it uses a substrate and superstrate of lower relative permittivity. Moreover, the proposed antenna exhibits a very wide bandwidth, enabling operation over a wider range of frequencies and higher gain despite the greater implantation depth than in previous studies. No shorting pins or vias are utilized in the proposed antenna, eliminating additional losses and reducing design complexity.

3. Conclusions

An implantable antenna operating in the MedRadio, LTE700, GSM850, GSM900, and WMTS bands is presented. Compact dimensions of 15 × 15 × 2.25 mm^3 are achieved by employing two meandering strip lines as the radiator element and ground plane. To clarify the biocompatibility requirement for practical application, the proposed implantable antenna is measured in a skin-mimicking gel for the MedRadio 402 band. The results indicate that the proposed antenna has a wide measured impedance bandwidth of 1035 MHz, ranging from 376 to 1411 MHz and covering the MedRadio, LTE700, GSM850, GSM900, and WMTS bands. A resonant frequency shift occurs when the proposed antenna is immersed in different biological tissues. Furthermore, the frequency response is insensitive to changes in the biological tissue temperature. The gain of the antenna is greater than −35 dBi when it is placed in the skin-mimicking gel. Owing to these features, the proposed implantable antenna is promising for application in implanted systems.

Acknowledgments

This work was sponsored by the Ministry of Science and Technology of the Republic of China under grant MOST 108-2221-E-239-004.

References

1 D. Halperin, T. Kohno, T. Heydt-Benjamin, K. Fu, and W. Maisel: IEEE Pervasive Comput. **7** (2008) 30. https://doi.org/10.1109/MPRV.2008.16
2 Federal Communications Commission: Medical Device Radiocommunications Service (MedRadio) (FCC, Sep. 2007), http://www.fcc.gov
3 International Telecommunications Union-Radiocommunications (ITU-R): Radio Regulations, Section 5.138 and 5.150, http://itu.int/home
4 W. C. Liu, F. M. Yeh, and M. Ghavami: Microw. Opt. Technol. Lett. **50** (2008) 2407. https://doi.org/10.1002/mop.23649
5 C. M. Lee, T. C. Yo, C. H., Luo, C. H. Tu, and Y. Z. Juang: Electron. Lett. **43** (2007) 660. http://doi.org/10.1049/el:20070463
6 C. R. Liu, Y. X. Guo, and S. Q. Xiao: IEEE Antennas Wireless Propag. Lett. **11** (2012) 1646. http://doi.org/10.1109/LAWP.2013.2237879
7 H. V. Prabhakar, U. K. Kummuri, R. M. Yadahalli, and V. Munnappa: Electron. Lett. **43** (2007) 848. https://doi.org/10.1049/el:20070688
8 R. Hossa, A Byndas, and M. E. Bialkowski: IEEE Microw. Wireless Compon. Lett. **14** (2004) 283. http://doi.org/10.1109/LMWC.2004.828007
9 C. Gabriel, S. Gabriel, and E. Corthout: Phys. Med. Biol. **41** (1996) 2231. https://doi.org/10.1088/0031-9155/41/11/001
10 T. Karacolak, A. Z. Hood, and E. Topsakal: IEEE Trans. Microw. Theory Tech. **56** (2008) 1001. http://doi.org/10.1109/TMTT.2008.919373
11 F. Fu, X. Xin, and W. Chen: Int. J. Hyperthermia **30** (2004) 56. http://doi.org/10.3109/02656736.2013.868534
12 Y. E. Yamac and S. C. Basaran: Int. J. RF Microw. Comput. Aided Eng. **30** (2020) e22406. https://doi.org/10.1002/mmce.22406
13 I. A. Shah, M. Zada, and H. Yoo: IEEE Trans. Antennas Propag. **67** (2019) 4230. https://doi.org/10.1109/TAP.2019.2908252
14 K. Yeap, C. Voon, T. Hiraguri, and H. Nisar: Microw. Opt. Technol. Lett. **61** (2019) 2105. https://doi.org/10.1002/mop.31871
15 M. Usluer, B. Cetindere, and S. C. Basaran: Microw. Opt. Technol. Lett. **62** (2020) 1581. https://doi.org/10.1002/mop.32185
16 J. Shang, Y. Yu1, and L. Xu: Microw. Opt. Technol. Lett. **62** (2020) 322. https://doi.org/10.1002/mop.32009

About the Authors

Pei-Jung Tseng received her B.S.M.T. degree from Fooyin University, Taiwan, in 2007 and her M.S. degree from Graduate Institute of Biomedical Sciences, College of Medicine, Chang Gung University, Taiwan, in 2009. Since 2020, she has been a medical laboratory scientist of the Department of Pathology and Laboratory Medicine, Taichung Veterans General Hospital, Taiwan. Her research interests are in bioscience. (elenatseng0902@gmail.com)

Ching-Fang Tseng received her Ph.D. degree in electrical engineering from Cheng Kung University, Tainan, in 2007. Currently, she is a professor in the Electronic Engineering Department, National United University, Taiwan. She has been involved in the research and development of wearable and flexible antennas, implantable antennas, biomedical devices, microwave/mm-wave/sub-THz mobile antennas, wireless biosensors, glass-free ULTCC and LTCC microwave dielectric materials, biomedical signal analysis, nonintrusive biological signal measurement, and intelligent health monitoring systems. (cftseng@nuu.edu.tw)

Xiang-Yi Zeng received his B.E. degree from the Electronic Engineering Department, National United University (NUU), Miaoli, Taiwan, in 2020 and is currently working toward his M.S. degree in electronic engineering at NUU. His main research direction is the development of wireless communication antennas. (a0955609786@gmail.com)

Cheng-Hsing Hsu received his B.S. degree in electronic engineering from Fu Jen Catholic University, Taipei, Taiwan, in 1997 and his M.S. and Ph.D. degrees in electrical engineering from National Cheng Kung University, Tainan, Taiwan, in 1999 and 2003, respectively. From 2003 to 2005, he worked as a principal engineer with the Nano-Device Research Department, Macronix International Co., Ltd., where he was engaged in novel nonvolatile memory materials and devices technology. In February 2005, he joined the Faculty of the Department of Electrical Engineering, Da-Yeh University, Chang-Hua, Taiwan. In August 2005, he became an assistant professor of the Department of Electrical Engineering, National United University, Miaoli, Taiwan, where in 2008 he became an associate professor and in 2013 a professor. His research interests include dielectric ceramics, thin film technology, planar antenna design, microwave passive components, nonvolatile memory devices, thermoelectric materials, and optoelectronic materials. (hsuch@nuu.edu.tw)

Ming-Hao Chou received his B.E degree in electronic engineering from National United University, Miaoli, Taiwan, in 2014 and his M.S. degree from the Electronic Engineering Department, National Taiwan University of Science and Technology, Taipei, Taiwan, in 2016. He is currently a high-frequency engineer working for Jess-Link Corporation. His research interests are in high-frequency device design, bioengineering, and sensors. (hf123456m@gmail.com)